TESLA-Report 1998-01

CEA/DAPNIA/SEA-98-02

RF steering experiments on TTF

Stéphane Fartoukh
CEA, DAPNIA/SEA
CE-Saclay F-91191 Gif/Yvette Cedex, France

January 27, 1998

Abstract

The aim of this paper is to propose a series of experiments capable of estimating the beam steering effects induced by the input couplers of TESLA cavities. After some recalls of beam dynamics, we will discuss the proposed method and give some results obtained by simulation.

1 Introduction

In addition to wakefield and chromatic effects, rf deflections of beams (i.e. transverse deflections of beams induced by radial asymmetries of the accelerating rf field around the beam axis) constitute a source of emittance dilution in linear colliders. Such a deflection of the beam centroid can be easily measured by the BPMs all along the linac and compensated for by dipole magnets and fast kickers; the difficulty comes from the non-uniformity of these deflections over the finite bunch length inducing emittance growth which cannot be controlled by the correction schemes usually used.
There are two main sources of rf deflections:

- the misalignments of the accelerating structures. Transverse cavity offsets create rf deflections due to rf focusing at low energy (i.e. when the average energy gain of the beam across the structure is comparable to its input energy). Tilted cavities (i.e. rotated around the horizontal or vertical axis) are responsible for a transverse Laplace force which takes non-zero values on the beam axis and deflects the particles depending on their relative position within the bunch.

- due to the HOM and input couplers, the intrinsic cylindrical symmetry of the accelerating structures is broken and, as a result, the beam is subjected to a rf kick at the exit of each cavity.

As we will see it, these kicks have roughly the following form:

$$\delta x'(z) = T\,\frac{q\,G_{\rm rf}}{E(z)}\,\cos(\phi_{\rm rf} - 2\pi f_{\rm rf}\,z/c - \phi_0) \tag{1}$$

where the notations used are described hereafter.

- q is the particle charge, z is its relative position within the bunch ($z = 0$ at the bunch center and $z > 0$ at the bunch tail) and $E(z)$ represents the particle energy at the cavity exit.

- $G_{\rm rf}$ [V/m], $f_{\rm rf}$ and $\phi_{\rm rf}$ denote the average accelerating gradient within the structure, the rf frequency and the rf phase respectively.

- T [rad] and ϕ_0 are constants which depend only on the type of the deflection considered (cavity misalignments or coupler effects).

Cavity misalignments give only an in-phase component of the transverse rf kick (i.e. $\phi_0 = 0$); at the opposite and as we will see it, rf deflections induced by the HOM and input couplers contain an out-of-phase component which may strongly contribute to emittance dilution (see Fig. 1).
After some recalls of beam dynamics, we will simulate and propose here a series of experiments based on measurements with beam in the TTF linac with the aim of estimating the value of the "T factor" (see Eq. 1) relative to the dipole asymmetry of the accelerating field induced by the cavity couplers.

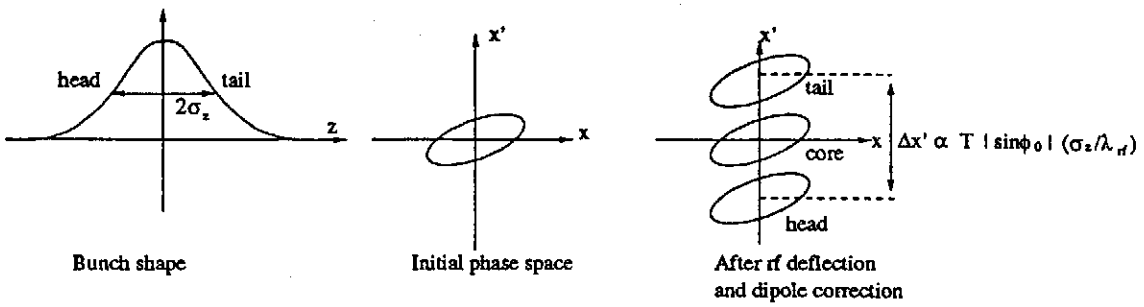

Figure 1: Beam filamentation due to rf deflection (case $\phi_{\rm rf} = 0$)

2 rf deflection due to cavity misalignments

2.1 Equation of motion in an accelerating cavity

We begin the discussion by writing the radial electromagnetic force affecting the trajectory of an ultra-relativistic charged particle ($v \sim c$) and due to the transverse electromagnetic fields existing in a axi-symmetric accelerating cavity. In terms of the on-axis longitudinal electrical field, $\tilde{E}_s(s,z) = E_s(s, t = (s+z)/c)$, seen by a particle at the abscissa s along the beam line and at a relative position z within the bunch and for particles closed to the structure axis, this force reads [1]

$$\vec{F}_\perp(s,z) = -\frac{q}{2}\frac{\partial \tilde{E}_s}{\partial s}\vec{r}(s,z) \tag{2}$$

where $\vec{r}(s,z)$ defines the transverse coordinates of the particle. Now, if $\gamma(s,z)\,mc^2$ represents the energy of the particle considered, we have also

$$q\frac{\partial \tilde{E}_s}{\partial s} = mc^2\,\gamma''(s,z) \tag{3}$$

where the derivative is taken with respect to s. The equation of motion of this particle within the structure is then (either in the horizontal plane or in the vertical plane)

$$x''(s,z) + \frac{\gamma'(s,z)}{\gamma(s,z)}\,x'(s,z) + \frac{\gamma''(s,z)}{2\,\gamma(s,z)}\,x(s,z) = 0 \tag{4}$$

with

$$\gamma'(s,z) = \frac{2\,q\,G_{\rm rf}}{mc^2}\,\cos\!\left(\omega_{\rm rf}\,s/c\right)\,\cos\!\left(\phi_{\rm rf} - \omega_{\rm rf}\,(s+z)/c\right) \tag{5}$$

for the TESLA cavities which are pure π-mode standing wave accelerating structures. In order to write this last equality, we have used the following conventions:

- $s = 0$ at the center of the fifth cell of the TESLA nine-cell structure, so that the on-axis longitudinal rf field seen by the bunch is maximum ($E_0^{max} = 2\,G_{\rm rf}$) at the center of each cell when $\phi_{\rm rf} = 0$.

- the on-axis longitudinal electrical field is $E_s(s,t) = 2\,E_0\,\cos\left(\omega_{\rm rf}\,s/c\right)\,\cos\left(\omega_{\rm rf}\,t\right)$ and the relation between the time t, the relative position z and the abscissa s along the cavity axis is $\omega_{\rm rf}\,t = \omega_{\rm rf}\,(s+z)/c - \phi_{\rm rf}$.

The solution of equation 4 is generally expressed in terms of R matrix:

$$X(s,z) \stackrel{\rm def}{=} \begin{pmatrix} x(s,z) \\ x'(s,z) \end{pmatrix} = R(s,z)\,X_0(z) \tag{6}$$

where $R(s,z)$ verifies the matricial differential equation

$$R'(s,z) = \begin{pmatrix} 0 & 1 \\ -\dfrac{\gamma'(s,z)}{\gamma(s,z)} & -\dfrac{\gamma''(s,z)}{2\gamma(s,z)} \end{pmatrix} R(s,z)\ . \tag{7}$$

An approximated solution of equation 7 is given by the so-called Chambers matrix [3],

$$R(L,z) = \begin{pmatrix} \cos\alpha - \sqrt{2}\,\cos\left(\phi_{\rm rf}(z)\right)\,\sin\alpha & \sqrt{8}\,\dfrac{\gamma_{in}(z)}{\overline{\gamma'}(z)}\,\cos\left(\phi_{\rm rf}(z)\right)\,\sin\alpha \\ -\dfrac{\overline{\gamma'}(z)}{\gamma_{out}(z)}\left(\dfrac{\cos\left(\phi_{\rm rf}(z)\right)}{\sqrt{2}} + \dfrac{1}{\sqrt{8}\,\cos\left(\phi_{\rm rf}(z)\right)}\right)\sin\alpha & \dfrac{\gamma_{in}(z)}{\gamma_{out}(z)}\left(\cos\alpha + \sqrt{2}\,\cos\left(\phi_{\rm rf}(z)\right)\,\sin\alpha\right) \end{pmatrix} \tag{8}$$

where the notations used are the following:

- $\phi_{\rm rf}(z) \stackrel{\rm def}{=} \phi_{\rm rf} - \omega_{\rm rf}\,z/c$ is the rf phase seen by a particle which is at the relative position z within the bunch and $\overline{\gamma'}(z) \stackrel{\rm def}{=} q\,G_{\rm rf}\,\cos\left(\phi_{\rm rf}(z)\right)/(mc^2)$ represents the average of the function $\gamma'(s,z)$ over the cavity length.

- $\gamma_{in}(z)\,mc^2$ and $\gamma_{out}(z)\,mc^2 = \left(\gamma_{in}(z) + \overline{\gamma'}(z)\,L\right)mc^2$ are the initial and final energy of the particle considered (L is the cavity length).

- $\alpha \stackrel{\rm def}{=} \dfrac{1}{\sqrt{8}\,\cos\left(\phi_{\rm rf}(z)\right)}\,\ln\left(\dfrac{\gamma_{out}(z)}{\gamma_{in}(z)}\right)$.

By solving numerically equation 7 and taking into account the effects of fringe fields (by an "hard-edge model" at the cavity input and output), we then obtain an R matrix which is very closed, even at low energy, to the Chambers matrix given here above. Note simply that the Chambers matrix is an even function of the rf phase (more precisely $R(z=0,\,\phi_{\rm rf}) = R(z=0,\,-\phi_{\rm rf})$) whereas the solution obtained by numerical integration of the equation of motion is not exactly (the function $\gamma(z=0,\,s)$ depending not symmetrically on the rf phase, see Eq. 5). For this reason, the simulation results which will be illustrated later are based on a numerical resolution of equation 7.
All the same, we will retain from now on that the focusing effects in accelerating structures are quasi-independent of the sign of the rf phase.

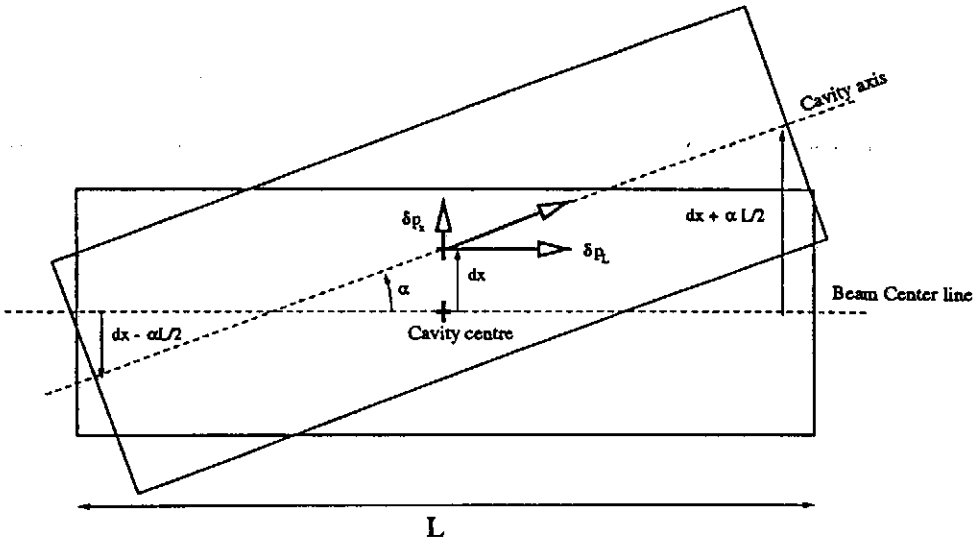

Figure 2: Scheme of a misaligned cavity

2.2 Effects on beam of a misaligned structure

Let us consider now a cavity misaligned with respect to the reference beam line. On Fig. 2, this one has been globally translated horizontally by a quantity dx; then, it has been rotated by an angle α around the vertical axis passing by its center. At the cavity exit, the bunch has then be subjected to an offset and to a kick given by the following expression:

$$\delta X \stackrel{\text{def}}{=} \begin{pmatrix} \delta x \\ \delta x' \end{pmatrix} = \begin{pmatrix} \alpha L/2 + dx \\ \alpha \end{pmatrix} + \left(\int_{-\infty}^{\infty} R(L,z)\, \rho(z)\, dz \right) \begin{pmatrix} \alpha L/2 - dx \\ -\alpha \end{pmatrix} \tag{9}$$

where $\rho(z)$ represents the longitudinal bunch distribution and where $R(L,z)$ is the cavity transfer matrix associated to a particle located at the relative position z within the bunch. In a regime where $\overline{\gamma'} L \ll \gamma_{in}$, the rf focusing effect vanishes (R_{21} term) and the matrix $R(L,z)$ given by Eq. 8 takes the following expression:

$$R(L,z) = \begin{pmatrix} 1 - \dfrac{1}{2}\dfrac{\overline{\gamma'}(z)\, L}{\gamma_{in}(z)} & L \\ 0 & 1 - \dfrac{1}{2}\dfrac{\overline{\gamma'}(z)\, L}{\gamma_{in}(z)} \end{pmatrix} + o\left(\frac{\overline{\gamma'} L}{\gamma_{in}}\right) \tag{10}$$

so that, by reconsidering the relation 9, we obtain for this regime

$$\delta X \overset{\overline{\gamma'} L \ll \gamma_{in}}{\sim} \frac{q\, G_{\text{rf}}\, L\, \cos\phi_{\text{rf}}}{2\, E_{in}} \begin{pmatrix} dx - \alpha L/2 \\ \alpha \end{pmatrix} . \tag{11}$$

where E_{in} is the beam energy at the cavity entrance.

3 rf deflection due to TESLA structure asymmetries

We discuss now the rf deflections of beams due to TESLA structure asymmetries induced by the input and HOM couplers. Insofar as the HOM couplers are quasi-uncoupled to the rf power transported by the accelerating fundamental mode, their effects on beam are negligible compared to the ones generated by the input coupler located at the cavity exit. At the input coupler location, a particle at a relative position z within the bunch is then subjected to a transverse kick $\delta x'(z)$ which is in quadrature with the accelerating field (Panowski Wenzel theorem), is proportional to the gradient $G_{\rm rf}$ and depends on the distance s_0 from the center of the end-cell to the center of the input coupler [2], $s_0 = 10.1$ cm for the TESLA cavities:

$$\begin{aligned} \delta x'(z) &= T\,\frac{q\,G_{\rm rf}}{E_{out}(z)}\,\sin\Big(\omega_{\rm rf}\,s_0/c - \phi_{\rm rf}(z)\Big) \\ &= \frac{q\,G_{\rm rf}}{E_{in}(z) + q\,G_{\rm rf}\,L\,\cos\Big(\phi_{\rm rf}(z)\Big)}\,\cos\Big(\phi_{\rm rf}(z) - \phi_0\Big) \end{aligned} \tag{12}$$

where $\phi_0 \stackrel{\rm def}{=} \omega_{\rm rf}\,s_0/c - \pi/2 \sim 67.7°$ for the TESLA structures. Finally, at high energy, the dependence of this rf kick becomes cosine-like with the rf phase and takes the following form:

$$\delta x'(z) = T\,\frac{q\,G_{\rm rf}}{E(z)}\,\cos\Big(\phi_{\rm rf}(z) - \phi_0\Big) \tag{13}$$

where $E(z)$ is the energy of the particle considered, say at the cavity center.

4 Experimental program of RF steering measurement in TTF and simulation results

We propose here a series of experiments in order to estimate the "T factor" associated to each of the eight accelerating cavities of the first cryomodule ACC1 of the TTF linac. The idea is the following [2]:

- select one of the cavities of the first cryomodule and detune the others.
- keep the accelerating gradient $G_{\rm rf}$ constant and vary the rf phase $\phi_{\rm rf}$ in the selected cavity.
- monitor the change in the beam position just before the first doublet.

This experiment has to be carried out with the low charge injector (injector I) in order to minimized the effects of wakefields (the relevant beam parameters used to simulate this experiment are the bunch length σ_z, the bunch charge Q_b and the initial particle energy E_{in} taken equal to 1 mm, 8/216 $\sim$ 0.037 nC and 12.511 MeV respectively). Fig. 3 shows the variation of the horizontal beam position at the BPM location (9.95 cm downstream

the first cryomodule) as a function of the rf phase in the selected cavity, the accelerating gradient being chosen equal to 15 MeV/m. As expected, the effects on beam of a tilted cavity are approximatively invariant if the rf phase of the cavity considered is changed into its opposite (dashed lines); therefore, the slopes at $\phi_{\rm rf} = 0$ of the curves obtained (solid lines) by adding the coupler effects (dot-dashed lines) and the ones generated by the cavity tilts are directly proportional to the factor $T \cdot \sin\phi_0$. More precisely, let us note $\delta x_i(\phi_{{\rm rf}_i})$ the variation of the horizontal beam displacement at BPM location with respect to the rf phase $\phi_{{\rm rf}_i}$ of cavity number i (solid line of the $i^{\rm th}$ curve of Fig. 3); by neglecting the finite bunch length and using Eq. 12, we obtain

$$\left(\frac{d\delta x_i}{d\phi_{{\rm rf}_i}}\right)_{\phi_{{\rm rf}_i}=0} = \frac{q\,G_{\rm rf}\,L_i}{E_{out}}\;T\,\sin\phi_0 \tag{14}$$

where L_i represents the distance from the input coupler of the cavity considered to the BPM and where E_{out} is the bunch energy at the exit of cavity number i.
The same experiment can be carried out with the third cryomodule (cavities number 17 to 24). Fig. 4 shows the results obtained in a situation similar to the last one, the only change being the higher energy E'_{in} at the entrance of module ACC3, $E'_{in} = E_{in} + 16 \times L_{\rm cav} \times G_{\rm rf} \sim 260$ MeV assuming the beam to be accelerated on crest at 15 MeV/m in the sixteen cavities of modules ACC1 and ACC2. As announced by equations 11 and 13, the curves obtained possesses a cosine-like behavior with the rf phases $\phi_{{\rm rf}_i}$ of the selected cavities but the measurement sensitivity is much lower since the input energy E'_{in} is about twenty times greater than E_{in}. More precisely, using the relations 11 and 13 and the preceding notations, we have

$$\begin{aligned}\delta x_i(\phi_{{\rm rf}_i}) \;=\; \frac{q\,G_{\rm rf}}{E'_{out}}\Big[\big(dx_i\,L_{\rm cav}/2 + \alpha_i\,L_{\rm cav}/2\,(L_i - L_{\rm cav}/2) + L_i\,T\,\cos\phi_0\big)\;\cos\phi_{{\rm rf}_i} + \\ L_i\,T\,\sin\phi_0\;\sin\phi_{{\rm rf}_i}\Big]\;,\; i = 17\ldots 24\end{aligned} \tag{15}$$

where dx_i and α_i represent the horizontal misalignment and the tilt of cavity number i and where $E'_{out} \sim E'_{in}$ is the bunch energy at the exit of the third module. Thus, the factor $T \cdot \sin\phi_0$ can be simply estimated by an antisymmetrization of the data obtained (sine part of Eq. 15).
In the case where the beam transport at low energy would pose problems, the measurement of the factor $T \cdot \sin\phi_0$ associated of each cavity of module ACC1 becomes difficult. Nevertheless, since it depends only on the geometry of the accelerating structures, we can suppose that its value is approximatively the same for all the cavities of the first module. Therefore, by monitoring the beam position as a function of the rf phase of the eight cavities of the first cryomodule all assumed to be tuned with an accelerating gradient of 15 MeV/m, the latter can be estimated in a same way as before. Fig. 5 illustrates this situation with the same beam parameters as the ones previously chosen. At the BPM

location, the transverse beam displacement has the following form

$$\delta x\left(\phi_{\mathrm{rf}}\right) \equiv \underbrace{f\left(\phi_{\mathrm{rf}}\right) T \cos(\phi_{\mathrm{rf}}-\phi_0)}_{\text{coupler effect}} + \underbrace{\sum_{i=1}^{8}\left\{g_i\left(\phi_{\mathrm{rf}}\right) dx_i + h_i\left(\phi_{\mathrm{rf}}\right)\alpha_i\right\}}_{\text{effect of the cavity misalignments}} + \underbrace{\xi_{\mathrm{BPM}}}_{\text{BPM misalignment}}$$

$$= f\left(\phi_{\mathrm{rf}}\right) T \cos(\phi_{\mathrm{rf}}-\phi_0) + \sum_{i=1}^{8}\left\{\underbrace{\left(g_i\left(\phi_{\mathrm{rf}}\right)-g_i(0)\right)}_{\stackrel{\mathrm{def}}{=}\tilde{g}_i(\phi_{\mathrm{rf}})} dx_i + \underbrace{\left(h_i\left(\phi_{\mathrm{rf}}\right)-h_i(0)\right)}_{\stackrel{\mathrm{def}}{=}\tilde{h}_i(\phi_{\mathrm{rf}})}\alpha_i\right\} + \mathrm{Cst} \tag{16}$$

where the functions f, g_i and h_i, $i = 1 \ldots 8$, are even functions of the rf phase. On Fig. 5 the bullets illustrates the behavior of the function $f\left(\phi_{\mathrm{rf}}\right) \cdot T \cdot \cos(\phi_{\mathrm{rf}} - \phi_0)$ whereas the errors bars corresponds to two times the RMS value of the function $\sum_{i=1}^{8}\{\tilde{g}_i\left(\phi_{\mathrm{rf}}\right) dx_i + \tilde{h}_i\left(\phi_{\mathrm{rf}}\right)\alpha_i\}$:

$$\sigma\left(\phi_{\mathrm{rf}}\right) = \left[\sum_{i=1}^{8}\tilde{g}_i^2\left(\phi_{\mathrm{rf}}\right)\right]^{\frac{1}{2}}\sigma_{dx} + \left[\sum_{i=1}^{8}\tilde{h}_i^2\left(\phi_{\mathrm{rf}}\right)\right]^{\frac{1}{2}}\sigma_{\alpha} \tag{17}$$

assuming the cavity misalignments are randomly distributed all along the line ($\sigma_{dx} \stackrel{\mathrm{def}}{=} \langle dx_i^2\rangle^{\frac{1}{2}}$ and $\sigma_{\alpha} \stackrel{\mathrm{def}}{=} \langle \alpha_i^2\rangle^{\frac{1}{2}}$, $i = 1 \ldots 8$). In other words, the curve experimentally obtained should be similar to the one given in Fig. 5, after the latter has been subjected to a global translation (the Cst term in Eq. 16) and some distortions, mainly at both extremities. Anyway, taking into account the parity of the functions occurring in Eq. 16, we have immediately

$$\left(\frac{d\delta x}{d\phi_{\mathrm{rf}}}\right)_{\phi_{\mathrm{rf}}=0} = -f(0)\, T \sin\phi_0 \tag{18}$$

where the factor $-f(0)$ depends only on the linac layout, the input beam energy E_{in} and the accelerating gradients G_{rf_i}, $i = 1 \ldots 8$, in the eight cavities of the first cryomodule. For $E_{in} = 12.511$ MeV and assuming the same accelerating gradient in the eight cavities of the first module, $G_{\mathrm{rf}} = 15$ MeV/m, we obtain numerically $f(0) = -6.5$ mm/(mrad·rad).

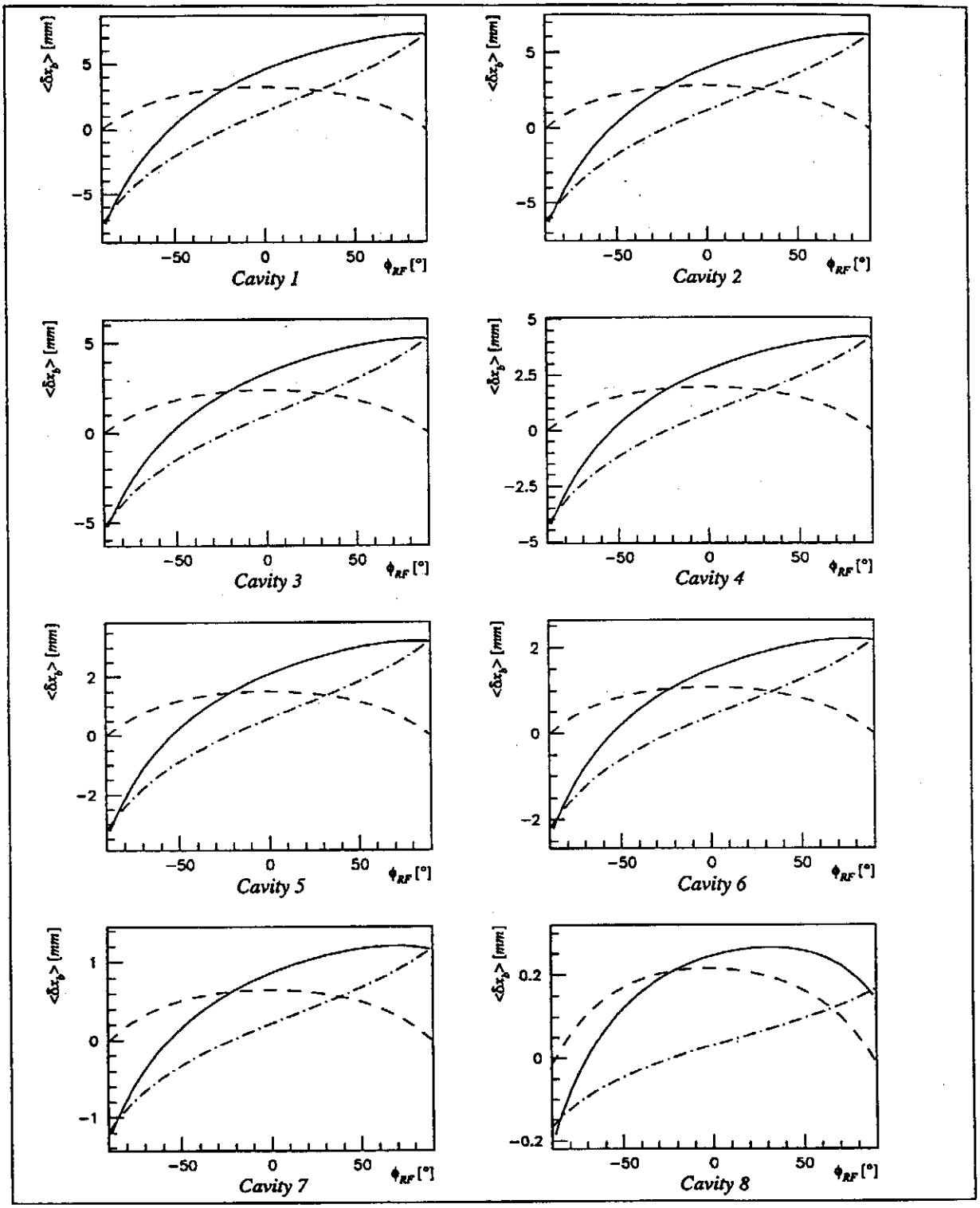

Figure 3: Horizontal beam displacement for a rf phase variation of one of the cavities of the first cryomodule; only tilt, α =1 mrad (dashed lines); only coupler effect, $T = 10/15 \sim 0.66$ mrad (dot-dashed lines); tilt + coupler (solid lines).

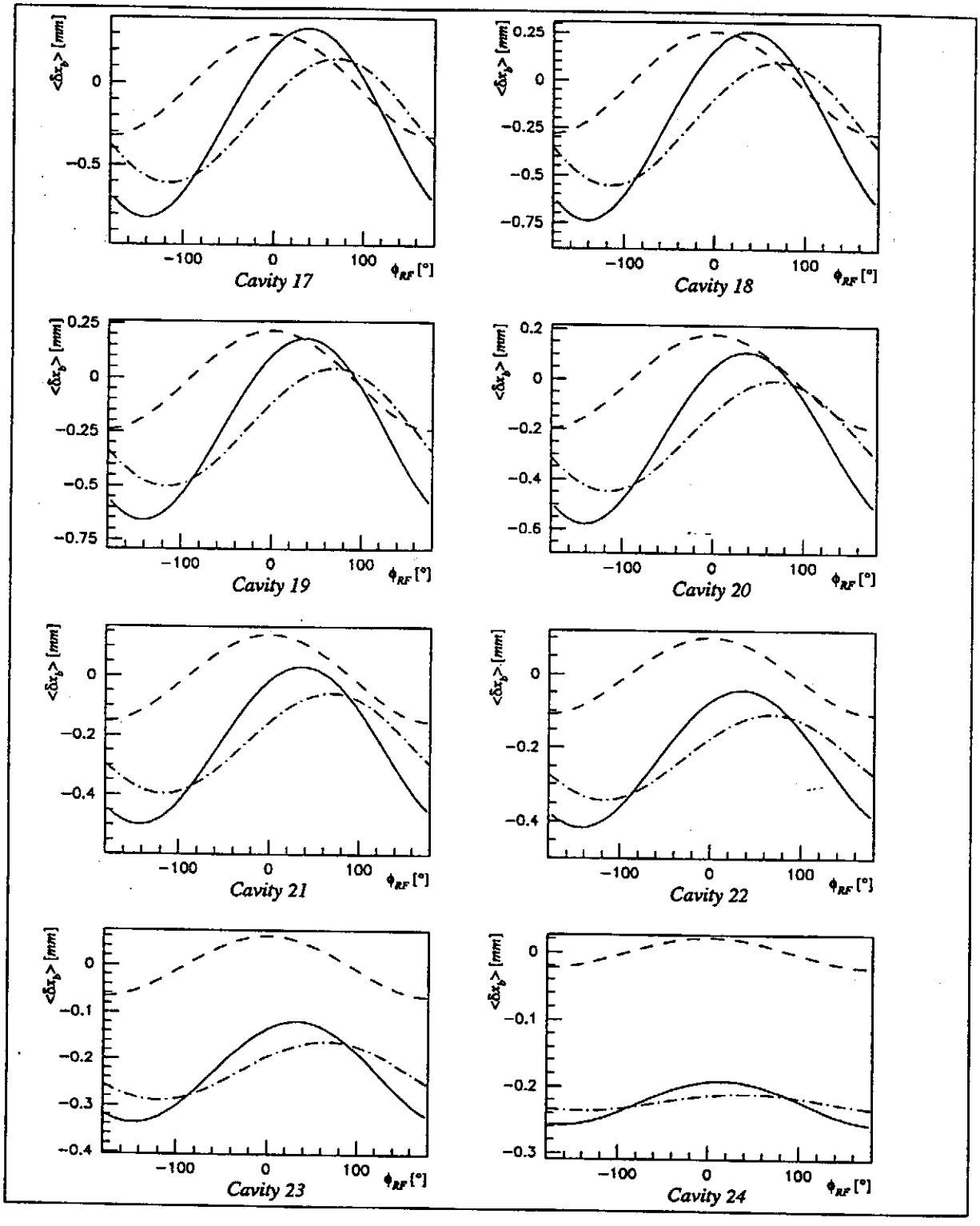

Figure 4: Horizontal beam displacement for a rf phase variation of one of the cavities of the third cryomodule; only tilt, α =1 mrad (dashed lines); only coupler effect, $T = 10/15 \sim 0.66$ mrad (dot-dashed lines); tilt + coupler (solid lines).

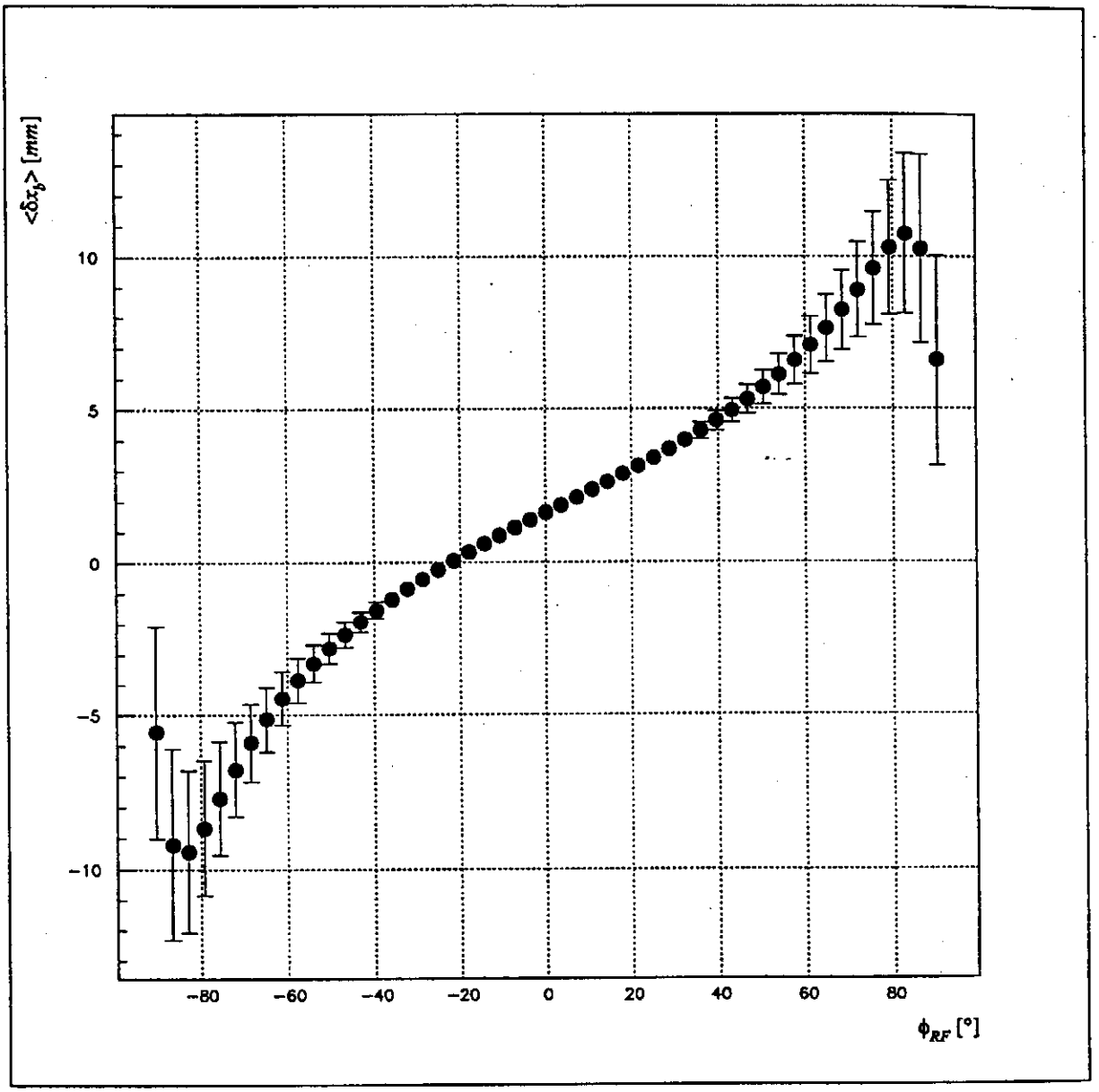

Figure 5: Horizontal beam displacement for a rf phase variation of all the cavities of the first cryomodule; only coupler effect, $T = 10/15 \sim 0.66$ mrad (bullets); statistics on the cavity misalignments (error bars), $\sigma_\alpha = 1$ mrad and $\sigma_{dx} = 0.5$ mm.

5 Conclusion

Using the first module (Fig. 3 or 5), the method seems then to be sensitive enough to measure the T factor with a resolution lower than 1 KeV/c (i.e. 66 μrad at $G_{rf} = 15$ MeV/m). These experiments are included in the calendar of the next TTF run (for April 1998) and the validity of this method will be checked against the experimental results obtained.

Acknowledgments

Thanks to A. Mosnier and O. Napoly for useful discussions and pertinent comments.

References

[1] K. J. Kim. Nucl. Instrum. Methods A **275**, 201 (1989).

[2] A. Mosnier. *Steering due to couplers.* Meeting TESLA TEST FACILITY, Orsay 1994, March 8-10.

[3] E. Chambers, Stanford High Energy Physics Laboratory Report (1965).